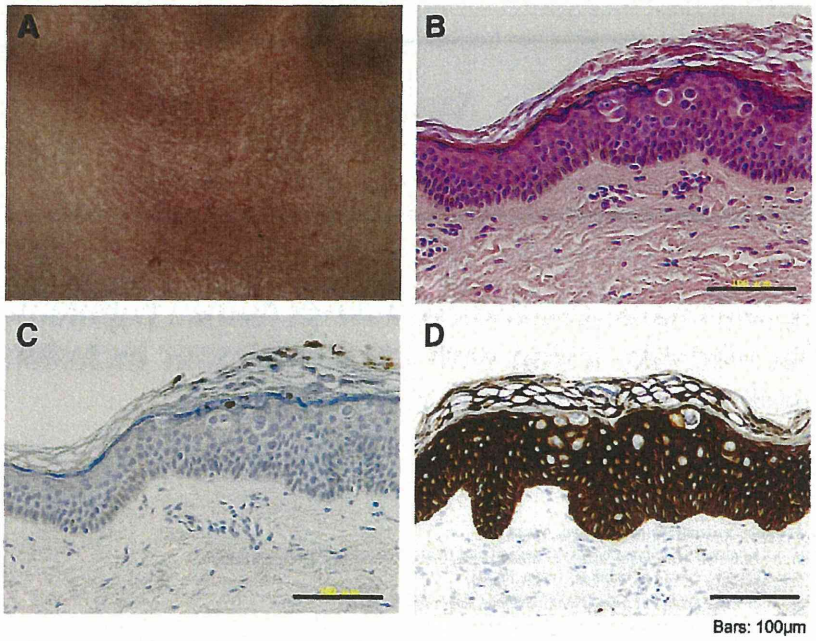

Fig. 1. Clinical (A), histopathological (B) and immunohistochemical (C and D) findings for the HPV 126-associated flat wart-like lesion. Macroscopic appearance of the flat wart-like lesions (A). In contrast to the normal skin adjacent to the flat wart-like lesion, Hg-ICBs are evident in balloon cells in the upper epidermal cell layers (B); strong positive signals for papillomavirus common antigen (L1 protein) in the nuclei of the cells in horny layer and cells with Hg-ICBs in granular layer (C); and positive signals for pan-cytokeratin are lacking in the cells with ICB (D). Scale bars; 100 μm.

like lesions separated by normal epidermis were included in the specimen. The epidermis showed mild acanthosis with basket-weave-like hyperkeratosis, partial hypergranulosis and mild papillomatosis, basic histological features compatible with those of flat warts (Fig. 1B) (Jablonska et al., 1985). However, additional unique histopathological features were also seen, i.e., keratinocytes with an enlarged nucleus, abundant blue-gray cytoplasm, occasional perinuclear haloes, and prominent keratohyalin granules observed in the granular and spinous layers, which are histopathological features consistent with EV (Jablonska and Orth, 1985). In addition, large clear cells contained homogeneous eosinophilic ICBs (Fig. 1B) resembling the homogeneous ICBs (Hg-ICBs) previously described in HPV 4/60/65-associated cutaneous warts (Egawa, 1994, 2005; Egawa et al., 1993).

Cloning and characterization of the HPV 126 genome

Although highly sensitive PCR failed to detect the DNA of either genus beta or mu papillomaviruses from the frozen biopsy specimen, a segment of a putative novel type genus gamma papillomavirus was amplified with a gamma papillomavirus-specific degenerate primers (Kawai et al., 2009) (Supplementary Fig. 1). Based on the nucleotide sequence, the full genome was cloned as described in Materials and methods. Sequencing of two clones from independent PCR reactions revealed the full genome consists of 7326 bp in length with a GC content of 50.5%. With a cutaneotropic papillomavirus primer set FAP59/FAP64 (Forslund et al., 1999), only the corresponding region of the cloned genome was amplified, further indicating the HPV is a single type in the lesions of this patient. The cloned HPV was found to be closely related to genus gamma papillomavirus types with an L1 ORF nucleotide similarity ranging from 60.1% to 68.7% (Table 1). According to the established criteria for a new type of papillomavirus that a new type should have 10% divergence of the L1 ORF nucleotide sequence from that of any other papillomavirus type {de Villiers, 2004 #16}, the cloned HPV qualified as a new type of papillomavirus designated as HPV126. According to the proposed criteria for species that should share between 60% and 70% nucleotide identity within a genus, we propose that HPV126, which has less than 70% nucleotide identity with any other papillomaviruses, constitutes a new species of genus gamma papillomavirus. Generation of a phylogenetic tree based on complete L1 nucleotide sequences of representative HPV types indicated that HPV 126 is most closely related to HPV 129 (Fig. 3), with similarity of 68.7% (Table 1). HPV 126 has a typical genomic organization for a genus gamma papillomavirus, and it has seven ORFs, E6, E7, E1, E2, E4, L2 and L1, but no E5 (Supplementary Fig. 2).

Immunohistochemical features of the wart lesions

Strong signals of L1 capsid proteins were seen in the nuclei of the cells in horny layer and cells with the ICBs in granular layer (Fig. 1C), suggesting active production of virions. In the cells with ICBs, little cytokeratin staining was observed while strong staining was observed in all epidermal cell layers of the lesions as well as its adjacent normal skin (Fig. 1D).

Table 1
Nucleotide sequence pairwise comparison of HPV 126 ORFs with those of representative genus gamma papillomaviruses.

ORF	E6	E7	E1	E2	E4	L1	L2
HPV type							
HPV 4	52.2	53.2	66.2	57.3	57.3	63.5	51.6
HPV 48	54.0	60.3	61.3	55.6	52.7	61.4	52.7
HPV 50	49.1	55.9	61.6	58.5	55.2	61.5	52.7
HPV 60	54.3	54.0	65.5	59.8	59.5	62.9	53.6
HPV 65	53.4	50.5	67.0	54.7	55.0	61.4	51.9
HPV 88	51.5	55.4	64.5	57.1	55.6	62.8	52.6
HPV 95	52.6	51.5	66.9	57.2	57.5	62.2	52.6
HPV 112	55.0	53.0	61.0	58.4	53.7	62.4	50.4
HPV 116	60.3	53.7	66.4	60.9	58.6	67.6	57.7
HPV 119	52.5	53.4	62.0	58.3	52.9	61.5	50.3
HPV 121	55.0	55.1	63.8	55.8	53.4	63.1	52.3
HPV 123	47.1	48.0	60.5	55.6	51.4	60.1	51.6
HPV 129	58.3	57.4	67.3	60.2	61.1	68.7	58.7

Similarities (%). Sequence for the genus gamma papillomaviruses were obtained from GenBank.

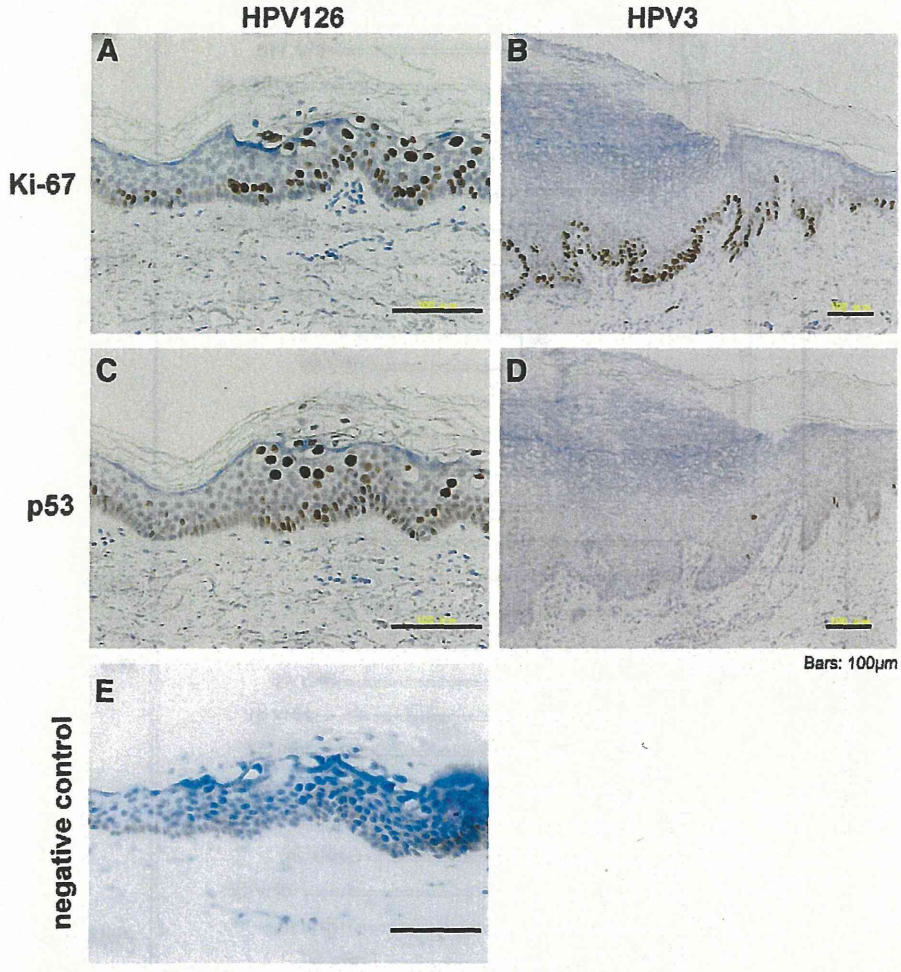

Fig. 2. Immunohistochemical features of the HPV 126-associated flat wart-like lesion. In contrast to the normal skin adjacent to the flat wart-like lesion (left side), positive signals for both Ki-67 (A) and p53 (C) are apparent in all compartments of the epithelium except for horny layer of the lesion (right side). However, a divergence is seen between Ki-67 and p53 staining. In contrast to that strong staining for Ki-67 is seen parabasal cells as well as cells of upper epidermal layers, the strong signal is seen predominantly in cells of upper epidermal cell layers. In contrast, weak (B) and faint (D) signals are restricted to the basal and parabasal (B) or lower spinous (D) layers of typical HPV 3-associated flat warts. Scale bars; 100 μm. As a negative control, no signals are observed in the staining of normal non-immune serum from the same source as the primary antibody (E).

Increased expression of Ki-67, an indicative marker of cycling cells, was observed in all compartments of the epithelium except for horny layer of the lesions, whereas its expression was restricted to the basal proliferative compartment of the adjacent normal epidermis (Fig. 2A) and to basal to parabasal cells in the typical HPV 3-positive flat warts (Fig. 2B).

Increased p53 staining was also observed in all compartments of the epithelium except for horny layer of the lesions in the HPV 126-associated lesions. However, unlike Ki-67, strong signals were not seen in parabasal cells for p53. In the adjacent normal epidermis, weak staining for p53 was restricted to the basal proliferative compartment (Fig. 2C), and faint staining was in the basal and lower spinous layers in HPV 3-positive typical flat warts (Fig. 2D). Five cases of typical HPV 3-associated flat warts were examined for comparison to confirm the unusual distribution of Ki-67 and p53 expression in the present flat wart-like lesion though the present case is the only patient with HPV 126-asssociated inclusion warts studied thus far. These observations are reminiscence of high grade cervical intraepithelial neoplasia. However, neither the HPV 126-associated flat wart-like lesions nor ordinary flat warts showed positive staining for $p16^{INK4a}$, while cervical cancer biopsy examined as a positive control exhibited strong positive signals (data not shown).

Discussion

In the present study, the full-length genome of a novel papillomavirus, HPV 126, was cloned from flat wart-like lesions arising in a Japanese ATL patient and characterized. The DNA genome of HPV 126 consists of 7326 base pairs and shows the gene arrangement characteristic for a cutaneous HPV. The nucleotide sequence of the L1 ORF of HPV 126 shares the highest homology of 68.7% to that of HPV 129, a genus gamma papillomavirus, thereby defining HPV 126 a novel type possibly constituting a novel species of the genus gamma papillomavirus (de Villiers et al., 2004). The HPV 126-associated cutaneous lesions on the chest, neck and extremities of our Japanese ATL patient were disseminated hypopigmented macules clinically resembling flat warts or tinea versicolor-like lesions seen in epidermodysplasia verruciformis (EV) and acquired EV patients (Jablonska and Orth, 1985; Lutzner et al., 1983).

On microscopy balloon cells with pale blue cytoplasm like those seen in flat wart-like lesions of EV or acquired EV patients (Jablonska and Orth, 1985; Lutzner et al., 1983). Additional features characteristic for the present case were ICBs most resemble those associated with HPV 4/60/65, which are members of species 1 (HPV 4/65) and species 4 (HPV 60) of genus gamma papillomaviruses. (Egawa,

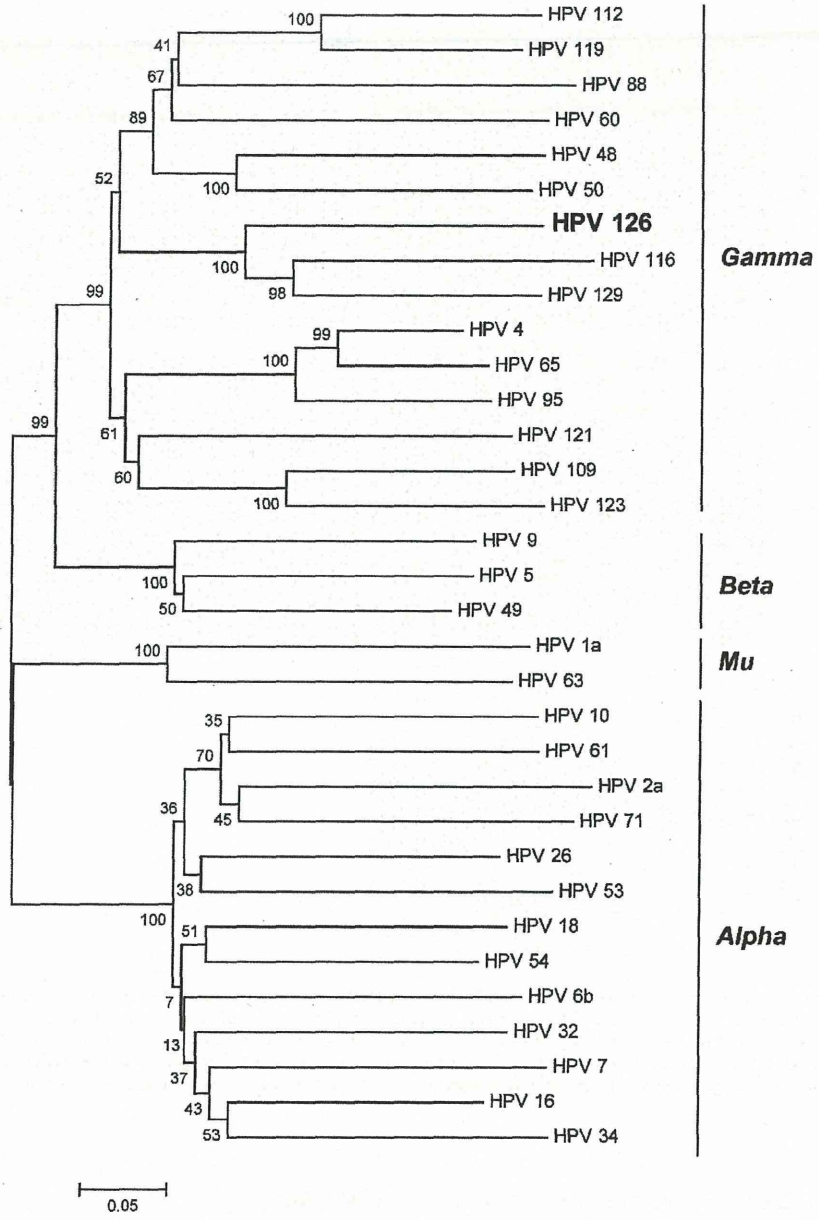

Fig. 3. Phylogenic relationships among HPV 126 and representative HPV types. A phylogenetic tree was constructed based on L1 ORF sequences using the neighbor-joining (NJ) method with 1000 bootstrap replicates. Numbers near branches indicate support index from NJ bootstrap percentage. Nucleotide sequences of representative HPVs were obtained from GenBank.

1994, 2005, 2007; Egawa et al., 1993). It is well known that distinct ICBs are pathognomonic for genus gamma and mu papillomaviruses (Egawa, 2007), although the histological features of recently isolated genus gamma papillomaviruses, including HPV 129 and HPV 116, have yet to be described (Bernard et al., 2010; Li et al., 2009). Cytokeratins were absent from cells containing Hg-ICBs (Fig. 1D), in which E4 proteins are thought to be a major component, though E4 protein expression was not examined in the present case. Thus like HPV16 E4 (Doorbar et al., 1989), HPV 126 E4 might be involved in interference with keratin filament assembly.

Another striking feature of the present case was its peculiar immunohistochemical localization of Ki-67 and p53, namely, they were expressed strongly and distributed in all compartments of the epithelium except for horny layer of the HPV 126-associated lesions (Fig. 2). Antigen Ki-67 is expressed during all phases of the cellular cycle, G1, S, G2, and M, of proliferating cells, but is absent in quiescent cells (G0). It is, therefore, a marker of cellular proliferation, which can be detected with monoclonal antibodies. Interaction of human papillomavirus oncoproteins E6 and E7 with cell cycle proteins leads to disturbance of the cell cycle and subsequent alteration in expression of some cell cycle proteins, such as $p16^{INK4a}$, cyclin D1, p53 and Ki-67. Abrupt inactivation of pRB can induce p53 accumulation though activation $p14^{ARF}$ (Bates et al., 1998). Like other HPVs, E7 protein of HPV 126 conserves the pRB binding motif and potentially inactivates pRB. Indeed some of the E7 proteins of cutaneous HPVs, such as HPV1 E7, can strongly bind and inactivate pRB (Hiraiwa et al., 1996; Schmitt et al., 1994). Thus it will be interesting to examine the activity of HPV 126 E7 protein and relationship among expression levels of HPV 126 E7, Ki-67 and the p53 accumulation. Unlike high grade CIN lesions where a positive correlation between the expression of the $p16^{INK4a}$

and Ki-67 has been reported (Nam et al., 2008; Queiroz et al., 2006), accumulation of $p16^{INK4a}$ was not detected in the Ki-67 positive cells (data not shown) in the present case whose clinical behavior and histopathological findings were benign (Kawai et al., 2009).

In conclusion, HPV 126, isolated and characterized in the present study, is a novel type of genus gamma papillomavirus and associated with flat wart- or EV-related tinea versicolor-like clinical features: histological ICBs as with other genus gamma papillomaviruses; and immunohistochemical expression of Ki-67 and p53 in characteristic manner not typical for benign cutaneous warts. It is probable that conditions accompanying immunosuppression in this ATL patient may have contributed to stimulate viral production of HPV 126, thus leading to wart formation, as known for acquired EV (Lutzner et al., 1983). To ascertain the true nature of HPV 126 and its associated warts, we need to perform epidemiological as well as further clinicopathological and virological studies on a larger number of lesions and patients, including immunocompromised individuals.

Materials and methods

Patient

A 56-year-old Japanese man was referred to us in August 2008 for evaluation of a 5-year history of disseminated hypopigmented macules clinically resembling flat warts or epidermodysplasia verruciformis-related tinea versicolor-like lesions (Jablonska and Orth, 1985) on the chest, neck, and extremities (Fig. 1A) (Kawai et al., 2009). The patient might have been suffering from immunodeficiency, because he was diagnosed as having chronic type of adult T-cell leukemia at the age of 52 years and manifested recurrent fungal pneumonia, rapidly progressing oral squamous cell carcinoma and multiple brain abscesses. A biopsy specimen was taken from the flat wart-like lesions with adjacent normal skin under suspicion of acquired EV (Lutzner et al., 1983). The biopsy specimen was cut into two pieces, one of which was fixed in 20% buffered formalin and embedded in paraffin for conventional histopathological and immunohistochemical analyses, and the other was frozen and stored in −70 °C for further analyses including DNA extraction.

Microscopical examination

Four-micrometer thick sections were obtained from the formalin-fixed and paraffin-embedded biopsy specimen, stained with hematoxylin and eosin (H&E), and examined microscopically.

Cloning and characterization of HPV DNA

Degenerate primers to detect genus gamma papillomaviruses were as described previously (Kawai et al., 2009). The amplified sequence turned out to correspond to nt 4641 to 5632 of the cloned HPV126 (Supplementary Fig. 1). Then abutting primers were designed juxtaposing the *HpaI* site present in the L1 region (forward primer: 5′-GTTAACAGTAGGCCATCCCTATTTTGATATTGTTG-3′, reverse primer: 5′-GTTAACAGTCTTTCAGTATTTGCATGAAAATAAATATCG-3′). The genome was amplified by 30 cycles of PCR using KOD plus DNA polymerase (Toyobo, Japan) according to the supplier's instruction; annealing at 60 °C, elongation at 68 °C for 8 min. About 8 kbp PCR products were purified and then cloned into pBluescriptIISK(−) (Stratagene, La Jolla, CA), in which 15-bp overlapping sequence of HPV 126 was added to the *NotI* site by PCR (forward primer: 5′-TGAAAGACTGTTAACGCGG-CCGCTCTAGAACTAGTGGATC-3′, reverse primer: 5′-TGGCCTACTGT-TAACGCGGCCGCCACCGCGGTGGAGCTCC-3′), by In-Fusion reaction (Clontech, Mountain View, CA). The complete genomic sequence of a clone was initially determined using primer walking by Nihon Gene Research Laboratories Inc. With the same set of primers (Supplementary Table 1), we confirmed the sequence of another clone from an independent PCR reaction to be identical (Supplementary Fig. 1). The DNA clone was submitted to the Human Papillomavirus Reference Laboratory (Heidelberg, Germany) for official designation, HPV 126, and the sequence was reconfirmed. HPV 126 sequence was submitted to DNA Data Bank of Japan (DDBJ) under accession number AB646346. Nucleotide sequence pairwise comparison of HPV 126 ORFs with types representing genus gamma papillomaviruses and L1 nucleotide global multiple sequence alignments were analyzed using ClustalW program (Thompson et al., 1994). Each gap was included and counted as one position. Phylogenetic analyses were conducted using MEGA version 4 (Tamura et al., 2007).

Immunohistochemical examination

Formalin-fixed and paraffin-embedded tissue sections (4 μm-thick) were deparaffinized in xylene and rehydrated through a series of graded ethanols (100–70%). For antigen retrieval, slides were immersed in citrate buffer (pH6.0) and were heated for 20 min in a microwave. The slides were then incubated in methanol containing 0.3% H_2O_2 to inhibit endogenous peroxidase activity. After washing, primary antibodies (Anti-papillomavirus common antigen, DAKO, clone K1H8, 1:200; Ki-67, DAKO, Clone MIB-1, 1:50; p53 protein, DAKO, Clone DO-7, 1:50; $p16^{INK4a}$, Santa Cruz, Clone JC8, 1:200; cytokeratin, Nichirei, polyclonal,1:2) were applied for 1 h and binding was detected using an Envision Kit (Dako Cytomation; K4006). Color development was achieved with 3, 3-diaminobenzine (DAB) as the chromogen and hematoxylin counterstaining was performed to aid in orientation. As a negative control, normal non-immune serum from the same source as the primary antibody was applied. Formalin-fixed, paraffin-embedded sections from an invasive uterine cervix squamous cell carcinoma biopsy served as a positive control for $p16^{INK4a}$.

Supplementary materials related to this article can be found online at doi: 10.1016/j.virol.2011.10.011.

Acknowledgments

Assignment of the HPV type number was kindly performed by Ethel-Michele de Villers, Human Papillomavirus Reference Laboratory, DKFZ, Heidelberg, Germany. We would like to express our appreciation to Takashi Yugawa, Tomomi Nakahara, and Shin-ichi Ohno for helpful discussions.

References

Bates, S., Phillips, A.C., Clark, P.A., Stott, F., Peters, G., Ludwig, R.L., Vousden, K.H., 1998. p14ARF links the tumour suppressors RB and p53. Nature 395, 124–125.
Bernard, H.U., Burk, R.D., Chen, Z., van Doorslaer, K., Hausen, H., de Villiers, E.M., 2010. Classification of papillomaviruses (PVs) based on 189 PV types and proposal of taxonomic amendments. Virology 401, 70–79.
de Villiers, E.M., Fauquet, C., Broker, T.R., Bernard, H.U., zur Hausen, H., 2004. Classification of papillomaviruses. Virology 324, 17–27.
Doorbar, J., Coneron, I., Gallimore, P.H., 1989. Sequence divergence yet conserved physical characteristics among the E4 proteins of cutaneous human papillomaviruses. Virology 172, 51–62.
Egawa, K., 1988. Another viral inclusion wart different from myrmecia. Nippon Hifuka Gakkai Zasshi 98, 1105–1112.
Egawa, K., 1994. New types of human papillomaviruses and intracytoplasmic inclusion bodies: a classification of inclusion warts according to clinical features, histology and associated HPV types. Br. J. Dermatol. 130, 158–166.
Egawa, K., 2005. Histochemical analysis of cutaneous HPV-associated lesions. Methods Mol. Med. 119, 27–40.
Egawa, K., 2007. Genus gamma- and mu-papillomaviruses: clinical and histopathological aspects suggestive of their important roles in virology and human pathology. Current Topics in Virology 6, 53–66.
Egawa, K., Delius, H., Matsukura, T., Kawashima, M., de Villiers, E.M., 1993. Two novel types of human papillomavirus, HPV 63 and HPV 65: comparisons of their clinical and histological features and DNA sequences to other HPV types. Virology 194, 789–799.
Forslund, O., Antonsson, A., Nordin, P., Stenquist, B., Hansson, B.G., 1999. A broad range of human papillomavirus types detected with a general PCR method suitable for analysis of cutaneous tumours and normal skin. J. Gen. Virol. 80 (Pt 9), 2437–2443.
Hiraiwa, A., Kiyono, T., Suzuki, S., Ohashi, M., Ishibashi, M., 1996. E7 proteins of four groups of human papillomaviruses, irrespective of their tissue tropism or cancer

association, possess the ability to transactivate transcriptional promoters E2F site dependently. Virus Genes 12, 27–35.
Honda, A., Iwasaki, T., Sata, T., Kawashima, M., Morishima, T., Matsukura, T., 1994. Human papillomavirus type 60-associated plantar wart. Ridged wart. Arch Dermatol 130, 1413–1417.
Jablonska, S., Orth, G., 1985. Epidermodysplasia verruciformis. Clin. Dermatol. 3, 83–96.
Jablonska, S., Orth, G., Obalek, S., Croissant, O., 1985. Cutaneous warts. Clinical, histologic, and virologic correlations. Clin. Dermatol. 3, 71–82.
Kawai, K., Egawa, N., Kiyono, T., Kanekura, T., 2009. Epidermodysplasia-verruciformis-like eruption associated with gamma-papillomavirus infection in a patient with adult T-cell leukemia. Dermatology 219, 274–278.
Li, L., Barry, P., Yeh, E., Glaser, C., Schnurr, D., Delwart, E., 2009. Identification of a novel human gammapapillomavirus species. J. Gen. Virol. 90, 2413–2417.
Lutzner, M.A., Orth, G., Dutronquay, V., Ducasse, M.F., Kreis, H., Crosnier, J., 1983. Detection of human papillomavirus type 5 DNA in skin cancers of an immunosuppressed renal allograft recipient. Lancet 2, 422–424.
Nam, E.J., Kim, J.W., Hong, J.W., Jang, H.S., Lee, S.Y., Jang, S.Y., Lee, D.W., Kim, S.W., Kim, J.H., Kim, Y.T., Kim, S., 2008. Expression of the p16 and Ki-67 in relation to the grade of cervical intraepithelial neoplasia and high-risk human papillomavirus infection. J Gynecol Oncol 19, 162–168.
Queiroz, C., Silva, T.C., Alves, V.A., Villa, L.L., Costa, M.C., Travassos, A.G., Filho, J.B., Studart, E., Cheto, T., de Freitas, L.A., 2006. Comparative study of the expression of cellular cycle proteins in cervical intraepithelial lesions. Pathol. Res. Pract. 202, 731–737.
Schmitt, A., Harry, J.B., Rapp, B., Wettstein, F.O., Iftner, T., 1994. Comparison of the properties of the E6 and E7 genes of low- and high-risk cutaneous papillomaviruses reveals strongly transforming and high Rb-binding activity for the E7 protein of the low-risk human papillomavirus type 1. J. Virol. 68, 7051–7059.
Tamura, K., Dudley, J., Nei, M., Kumar, S., 2007. MEGA4: Molecular Evolutionary Genetics Analysis (MEGA) software version 4.0. Mol. Biol. Evol. 24, 1596–1599.
Thompson, J.D., Higgins, D.G., Gibson, T.J., 1994. CLUSTAL W: improving the sensitivity of progressive multiple sequence alignment through sequence weighting, position-specific gap penalties and weight matrix choice. Nucleic Acids Res. 22, 4673–4680.

OPEN ACCESS Freely available online

PLOS ONE

A Novel Interaction between hScrib and PP1γ Downregulates ERK Signaling and Suppresses Oncogene-Induced Cell Transformation

Kazunori Nagasaka[1], Takayuki Seiki[1], Aki Yamashita[1], Paola Massimi[2], Vanitha Krishna Subbaiah[2], Miranda Thomas[2], Christian Kranjec[2], Kei Kawana[1], Shunsuke Nakagawa[3], Tetsu Yano[1], Yuji Taketani[1], Tomoyuki Fujii[1], Shiro Kozuma[1], Lawrence Banks[2]*

1 Department of Obstetrics and Gynecology, Faculty of Medicine, The University of Tokyo, Tokyo, Japan, **2** International Centre for Genetic Engineering and Biotechnology, Area Science Park, Trieste, Italy, **3** Department of Obstetrics and Gynecology, The Teikyo University School of Medicine, Tokyo, Japan

Abstract

Previous studies have shown that the cell polarity regulator hScrib interacts with, and consequently controls, the ERK signaling pathway. This interaction occurs through two well-conserved Kinase Interacting Motifs, which allow hScrib to bind ERK1 directly, resulting in a reduction in the levels of phospho-ERK. This suggests that hScrib might recruit a phosphatase to regulate this signaling pathway. Using a proteomic approach we now show that Protein Phosphatase 1γ (PP1γ) is a major interacting partner of hScrib. This interaction is direct and occurs through a conserved PP1γ interaction motif on the hScrib protein, and this interaction appears to be required for hScrib's ability to downregulate ERK phosphorylation. In addition, hScrib also controls the pattern of PP1γ localization, where loss of hScrib enhances the nuclear translocation of PP1γ. Furthermore, we also show that the ability of hScrib to interact with PP1γ is important for the ability of hScrib to suppress oncogene-induced transformation of primary rodent cells. Taken together, these results demonstrate that hScrib acts as a scaffold to integrate the control of the PP1γ and ERK signaling pathways and explains how disruption of hScrib localisation can contribute towards the development of human malignancy.

Citation: Nagasaka K, Seiki T, Yamashita A, Massimi P, Subbaiah VK, et al. (2013) A Novel Interaction between hScrib and PP1γ Downregulates ERK Signaling and Suppresses Oncogene-Induced Cell Transformation. PLoS ONE 8(1): e53752. doi:10.1371/journal.pone.0053752

Editor: Cara Gottardi, Northwestern University Feinberg School of Medicine, United States of America

Received January 29, 2012; **Accepted** December 4, 2012; **Published** January 24, 2013

Funding: This work was supported by research grants from the Okinaka Memorial Institute for Medical Research (to K.N.) and by a Grant-in-Aid for Scientific Research (no. 24592506, to K.N.) from the Ministry of Education, Science and Culture, Japan, and by research grants from the Associazione Italiana per la Ricerca sul Cancro and the Wellcome Trust (to L.B.). The funders had no role in study design, data collection and analysis, decision to publish, or preparation of the manuscript.

Competing Interests: The authors have declared that no competing interests exist.

* E-mail: banks@icgeb.org

Introduction

The control of cell polarity and the maintenance of tissue architecture are intimately related and are, in part, controlled by a tri-partite macromolecular signaling complex consisting of the Scrib complex, the Par complex and the Crumbs complex [1,2]. Through a series of antagonistic interactions the components of these three complexes control a variety of downstream signaling pathways that, in turn, directly contribute to the regulation of cell polarity and cell proliferation [3]. It is now clear that the loss of control of these pathways is a common event during the development of diverse human malignancies [1,4–7]. These defects are particularly evident at the later stages of malignant progression, and a variety of studies in both Drosophila and transgenic mice have provided additional supporting evidence of tumour suppressor activity for the various components of these signaling complexes [8–11].

The hScrib complex consists of three proteins, hScrib, hDlg1 and Hugl-1/2. In *Drosophila*, loss of either Scrib or Dlg produces imaginal disc overgrowth with invasive characteristics [8] [12], phenotypes that can be functionally complemented by the mammalian equivalents [13–15]. More recently Scrib has been implicated in the control of the JNK and ERK signaling cascades, and loss of hScrib appears to enhance the effects of the Ras and Myc oncogenes, and can contribute to mammary tumour development [16–21]. Recent studies have also demonstrated that hScrib can interact directly with ERK, and control both ERK activation and its nuclear translocation [19]. However, the physical interaction between ERK and hScrib is not sufficient to explain the inactivation of ERK, since high levels of hScrib appear capable of directly reducing the levels of ERK phosphorylation [19]. Since hScrib has no known phosphatase activity itself, it therefore seemed possible that a protein phosphatase might be recruited by hScrib to fully inactivate the ERK signaling pathway.

Control of ERK activation reflects an exquisite balance between the activities of the activating kinases and the de-activating protein phosphatases. Activated ERK can translocate to the nucleus, where it activates several transcription factors and also phosphorylates cytoplasmic and nuclear kinases [22–24]. Since phosphorylation of both the threonine and tyrosine residues of ERK is required for its activation, dephosphorylation of either is sufficient for its inactivation [25]. There are several reports demonstrating that dephosphorylation of active ERK can be achieved by tyrosine-specific phosphatases, by serine/threonine-specific phos-

phatases or by dual specificity (threonine/tyrosine) protein phosphatases [26–29]. One of the important negative regulators of the ERK signaling pathway is PP2A, a member of the PPP family of protein serine/threonine phosphatases which also includes PP1 [30,31]. However, PP2A is thought to exert its activity mainly upon other activating kinases within the cascade, rather than upon ERK itself [32–34]. In addition, recent studies have also shown that hScrib can directly regulate the Akt signaling cascade by recruitment of the protein phosphatase PHLPP1 to the plasma membrane, thereby resulting in de-phosphorylation of Akt [35]. Here, we have used a proteomic approach to extend our investigations into the regulation of the ERK signaling cascade by hScrib. We now show that hScrib interacts with PP1γ, and that this association correlates with the ability of hScrib to downregulate ERK activation. We also provide compelling evidence that hScrib directly contributes to the regulation of PP1γ function by controlling its translocation between the cytoplasm and the nucleus. Thus, loss of hScrib expression results in both ERK activation and aberrant nuclear translocation of PP1γ.

Materials and Methods

Cells and treatments

HEK293 (human embryonic kidney cells) and HaCaT (Human keratinocytes) were obtained from ATCC [36,37]. HEK293, HaCaT and Baby Rat Kidney (BRK) cells were cultured in Dulbecco's modified Eagle's medium (DMEM) supplemented with 10% fetal bovine serum, penicillin-streptomycin (100 U/mL) and glutamine (300 μg/mL) in a humidified 5%CO_2 incubator. Transfection was carried out using calcium phosphate precipitation as described previously [37] or using Lipofectamine 2000 (Invitrogen) according to the manufacturer's protocol. The depleted Scribble cell lines were generated as described previously [19]. Cell transformation assays were done using BRK cells obtained from 9 day old Wistar rats with a combination of HPV-16 E7 and EJ-ras, plus the appropriate hScrib and PP1γ expression plasmids. Cells were placed under G418 selection for three weeks, and then fixed and stained.

Plasmids

The wild type pCDNA3-HA-PP1γ was the kind gift of Dr. Wilhelm Krek (Swiss Federal Institute of Technology (ETH) Zurich). The wild type HA-tagged pcDNA hScrib expression plasmid and the truncated mutant pGEX hScrib PDZ1-C, PDZ1-4, S1445A, S1445D, and CT expression plasmids have been described previously [19]. The L1266Y1268→AA mutation (KADA) to doubly change the Leucine (L) and Tyrosine (Y) residues to Alanine (A) in hScrib was done using the QuikChange site-directed mutagenesis kit from Stratagene Cloning Systems (Celbio) according to the manufacturer's instruction. The mutants were confirmed by DNA sequencing. See Figure S1 for a detailed description of the location of the different hScrib mutations.

Antibodies

The following commercial antibodies were used at the dilution indicated: anti-hScrib goat polyclonal antibody (Santa Cruz, WB 1:1000), anti-PP1γ goat polyclonal antibody (Santa Cruz, WB 1:1000), anti-PP1γ sheep polyclonal antibody (Abcam, WB 1:1000), anti-p44/42 MAPK (Erk1/2) antibody (Cell Signaling Technology, WB 1:1000), anti-phospho p44/42 MAPK (Erk1/2) (Thr202/Tyr204) antibody (Cell Signaling Technology, WB 1:1000), anti-HA monoclonal antibody 12CA5 (Roche, WB 1:500), anti-γ-tubulin monoclonal antibody (Sigma, WB 1:5000), anti-p84 mouse monoclonal antibody (Abcam, WB 1:1000), anti-E-Cadherin rabbit polyclonal antibody (Santa Cruz, WB 1:500), anti-α-tubulin mouse monoclonal antibody (Abcam, WB 1:1000).

Immunofluorescence and Microscopy

For immunofluorescence cells were grown on glass coverslips and fixed in 3.7% paraformaldehyde in PBS for 20 mins at room temperature. After washing in PBS the cells were permeabilised in PBS/0.1% Triton for 5 mins, washed extensively in PBS and then incubated with primary antibody diluted in PBS for 1 hour followed by the appropriately conjugated secondary antibodies. Secondary antibodies conjugated to Alexa Fluor 488 or 548 were obtained from Invitrogen. The cells were then washed several times in water and mounted on glass slides. Cells were visualized by using a Zeiss Axiovert 100 M microscope attached to a LSM 510 confocal unit.

siRNA transfection

HEK293 cells were seeded on 6 cm dishes and transfected using Lipofectamine 2000 (Invitrogen) with control siRNA against Luciferase (siLuc), or siRNA against hScrib and PP1γ sequences (Dharmancon). 48 hours post-transfection cells were harvested and total cells extracts or cell fractionated extracts were then analysed by western blotting.

Fusion protein purification and in vitro binding assays

GST-tagged fusion proteins were expressed and purified as described previously [19]. Proteins were translated in vitro using the Promega TNT kit and radiolabelled with (^{35}S) cysteine or (^{35}S) methionine (Perkin Elmer). Equal amounts of in vitro-translated proteins were added to GST fusion proteins bound to glutathione agarose (Sigma) and incubated for 1 hour at 4°C. After extensive washing with PBS containing 0.25% NP-40, or as otherwise indicated, the bound proteins were analysed by SDS-PAGE and autoradiography.

In vitro phosphorylation

Purified GST fusion proteins were incubated with commercially purified ERK1 (Cell Signaling Technology) or PKA (Promega) for 20 mins at 30°C in phosphorylation buffer (0.25 M Tris pH7.5, 1 M $MgCl_2$, 3 M NaCl, 0.3 mM aprotinin, 1 mM Pepstatin) or using the kinase buffer supplied by New England Biolabs supplemented with 56 nM (^{32}P) γ-ATP (Perkin Elmer) and 10 mM ATP following the manufacturer's instruction. After extensive washing, the phosphorylated proteins were monitored by SDS-PAGE and autoradiography.

Mass spectrometry analysis

HEK293 cells were transfected with HA-tagged Scrib and after 24 hours the cells were extracted in mass spectrometry lysis buffer (50 mM Hepes pH 7.4, 150 mM NaCl, 50 mM NaF, 1 mM EDTA, 0.25% NP40) and extracts incubated with anti-HA beads (Sigma) for 2–3 hours on a rotating wheel at 4°C. The beads were then extensively washed with PBS, dried and the immunoprecipitated proteins were subjected to proteomic analysis as described previously [38].

Subcellular Fractionation assays

Differential extraction of HEK 293 cells to obtain cytoplasmic, membrane, cytoskeleton, and nuclear fractions was performed using the Calbiochem ProteoExtract Fractionation Kit according to the manufacturer's instructions. To inhibit phosphatase activity during the preparation of cell lysates, phosphatase inhibitors

A

log (e)+	#	total	HA-Scribble
-1189.3	91	200	SCRIB, scribble
-327.5	29	37	VIM, vimentin
-73.2	6	10	NPM1P21, nucleophosmin
-60.5	6	6	PPP1CC, protein phosphatase 1, catalytic subunit, gamma isoform
-59.6	6	6	NCL, nucleolin

ADLDKLNIDS IIQR [15]llev
LFEYGGFPPE SNYLFLGDYV DR [95]gkqs
IKYPENFFLL R [122]gnhe
YPENFFLLR [122]gnhe
AHQVVEDGYE FFAK [260]rqlv
KKPNATRPVT PPR [314]gmit

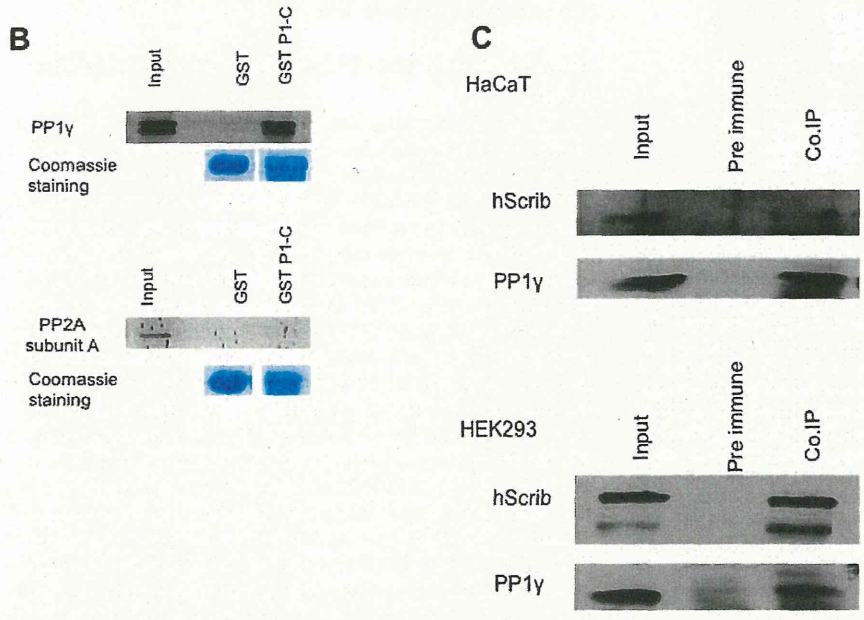

Figure 1. Interaction between hScrib and PP1γ in vivo. A) Results from the mass spectroscopy analysis of hScrib containing immunoprecipitates identified 6 peptides (indicated) corresponding to PP1γ. B) In vitro translated PP1γ (upper panels) and PP2A subunit A (lower panels) were incubated for 1 hour at 4°C with purified GST-hScribP1-C or GST alone immobilized on Glutathione agarose. After extensive washing, the bound proteins were analysed by SDS–PAGE and autoradiography which are shown in each of the upper panels. The gels were rehydrated and stained with Coomassie to show equal levels of GST loading in the respective lower panels. C) Endogenous PP1γ was immunoprecipitated from HaCaT (upper panels) and HEK 293 cells (lower panels), with pre-immune antibody used as control. The immunoprecipitated proteins were then analysed by western blotting using anti-hScrib and anti-PP1γ antibodies.
doi:10.1371/journal.pone.0053752.g001

(1 mM Na_3VO_4, 1 mM β-Glycerophosphate, 2.5 mM Sodium Pyrophosphate, 1 mM Sodium Fluoride) were also included.

Immunoprecipitation and Western blotting

Total cellular extracts were prepared by directly lysing cells from dishes in SDS lysis buffer. Alternatively cells were lysed in either E1A buffer (25 mM HEPES pH 7.0, 0.1% NP-40, 150 mM NaCl, plus protease inhibitor cocktail; Calbiochem) or RIPA buffer (50 mM Tris HCl pH 7.4, 1% NP-40, 150 mM NaCl, 1 mM EDTA, plus protease inhibitor cocktail; Calbiochem) and the cell extracts were analysed by SDS-PAGE and western blotting. For immunoprecipitations, total cell lysates were transferred into a tube of equilibrated EZview Red Anti-HA Affinity Gel beads (Sigma), and incubated for 2 hours at 4°C. Immunoprecipitates were extensively washed four times in lysis buffer and solubilised in SDS-PAGE sample buffer. For western blotting, 0.45 μm nitrocellulose membrane (Schleicher and Schuell) was used and membranes were blocked for 1 hour at 37°C in 10% milk/PBS followed by incubation with the appropriate primary antibody diluted in 10% milk/0.5% Tween 20 for 1 hour. After

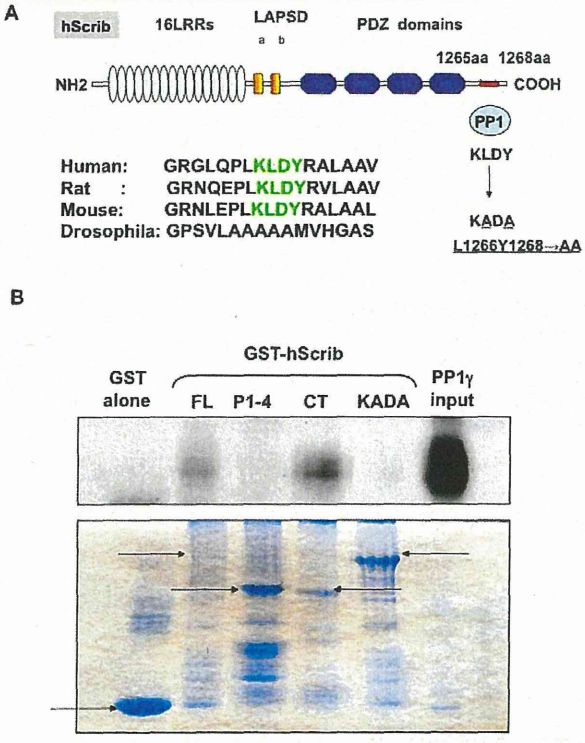

Figure 2. hScrib contains a consensus PP1-binding motif. A) The schematic shows the arrangement of the functional domains on the hScrib protein, highlighting the LRR, LAPSD and PDZ domains. The putative PP1-binding site, the RVXF (the consensus sequence is K/R/H/N/S V/I/L X F/W/Y) motif is also shown, where X is any amino acid. The hScrib mutant in which the PP1-binding site KLDY was mutated to KADA in order to disrupt the interaction with PP1 is shown. A comparison sequence alignment of the region of hScrib containing the PP1-binding motif indicating its absence in Drosophila also shown. B) In vitro translated and radiolabeled PP1γ was incubated with purified full length GST-hScrib fusion protein (FL), GST-hScrib PDZ1-4 (P1-4), GST-hScrib CT (CT), GST-hScrib L1266Y1268→AA (KADA) and GST alone as a control. After extensive washing the bound PP1γ was ascertained by SDS PAGE and autoradiography. The upper panel shows the autoradiograph, with the input of PP1γ also shown for comparison. The lower panel shows the Coomassie stain of the gel showing the levels of GST fusion protein loading, with the arrows indicating the relevant full length fusion proteins.
doi:10.1371/journal.pone.0053752.g002

several washings with PBS 0.5% Tween 20, secondary antibodies conjugated with HRP (DAKO) in 10% milk/0.5% Tween 20 were incubated for 1 hour. Blots were developed using Amersham ECL reagents according to the manufacturer's instructions.

Results

PP1γ is a direct binding partner of hScrib

Based on our previous studies we reasoned that down-regulation of ERK phosphorylation by hScrib might involve the recruitment of a protein phosphatase [19]. To investigate this possibility we performed proteomic analyses to identify additional interacting partners of hScrib. HEK293 cells were transfected with an HA-tagged hScrib expression plasmid and after 24 hours the cells were extracted, and hScrib–bound protein complexes were immunoprecipitated with anti-HA agarose beads and then subjected to mass spectroscopy analysis. Several previously reported interacting partners were identified, including vimentin. However, of the novel interacting partners, the most prominent phosphatase identified was the catalytic subunit of PP1γ (Figure 1A), a major eukaryotic serine/threonine protein phosphatase. To investigate whether hScrib can interact with PP1γ, an in vitro pull-down assay was performed using purified GST-hScrib P1-C fusion protein and in vitro translated radiolabeled PP1γ. For comparison a similar assay was also done using in vitro translated radiolabeled protein phosphatase 2A (PP2A). After extensive washing the bound PP1γ and PP2A were detected by SDS PAGE and autoradiography, and the results in Figure 1B demonstrate strong interaction between hScrib and PP1γ. In contrast, no interaction was observed between hScrib and PP2A, confirming the specificity of the association between hScrib and PP1γ. To determine whether endogenous hScrib and PP1γ could exist in a complex in vivo, immunoprecipitations were performed on cell extracts from HEK293 and HaCaT epithelial cells using anti-PP1γ antibody. Co-immunoprecipitated hScrib was then detected by western blotting, and the results in Figure 1C show a significant degree of co-immunoprecipitation of hScrib with PP1γ in both cell lines. Taken together, these results demonstrate that hScrib and PP1γ can exist as a complex in vivo.

hScrib interacts with PP1γ through a conserved RVxF motif

The PP1 holoenzyme is composed of a catalytic subunit and several regulatory subunits, which target the catalytic subunit to specific subcellular locations. The RVxF motif is a short conserved PP1-binding motif initially identified in previous studies showing that these residues can block the interaction of regulatory subunits with the PP1 catalytic subunit [39]. As shown in Figure 2A, analysis of the hScrib sequence reveals the presence of a putative PP1 binding motif, KLDY (the consensus sequence is: {K/R/H/N}.{S/V/I/L}.X.{ F/W/Y}) [40,41] spanning residues 1265–1268. This sequence is also highly conserved in mammalian Scrib proteins, but is absent in Drosphila. Based on previous studies, mutation of the L and Y residues would be expected to severely perturb the interaction with PP1 [39–42]. To investigate whether this KLDY motif is responsible for the capacity of hScrib to bind to PP1γ, a panel of GST-hScrib fusion proteins consisting of the full length (FL), two truncated proteins encompassing PDZ domains 1–4 (P1-4) and the carboxy terminal third of hScrib (CT), plus a full length hScrib with the KLDY/KADA mutation, were used in pull-down assays with in vitro translated radiolabeled PP1γ. The levels of bound PP1γ were then assessed by SDS PAGE and autoradiography and, as can be seen from Figure 2B, PP1γ binds to the carboxy terminal region of hScrib which contains the predicted PP1 binding motif. Furthermore the KLDY/KADA mutation significantly decreases the capacity of PP1γ to interact with hScrib, confirming that the major site of interaction is through the KLDY consensus motif.

hScrib and ERK are substrates of PP1γ

We have previously shown that hScrib is a substrate for both PKA and ERK. Furthermore, hScrib can downregulate ERK activation through a direct protein-protein interaction [19], although the precise mechanism by which hScrib can achieve this is still unknown. We therefore wanted to determine whether phosphorylation of hScrib by either PKA or ERK1 could influence the ability of hScrib to interact with PP1γ and, furthermore, whether hScrib itself was a substrate of PP1γ. To do this, purified GST-hScrib fusion protein was subject to phosphorylation by either PKA or ERK1 in the presence of non-radiolabeled ATP, and after extensive washing binding assays

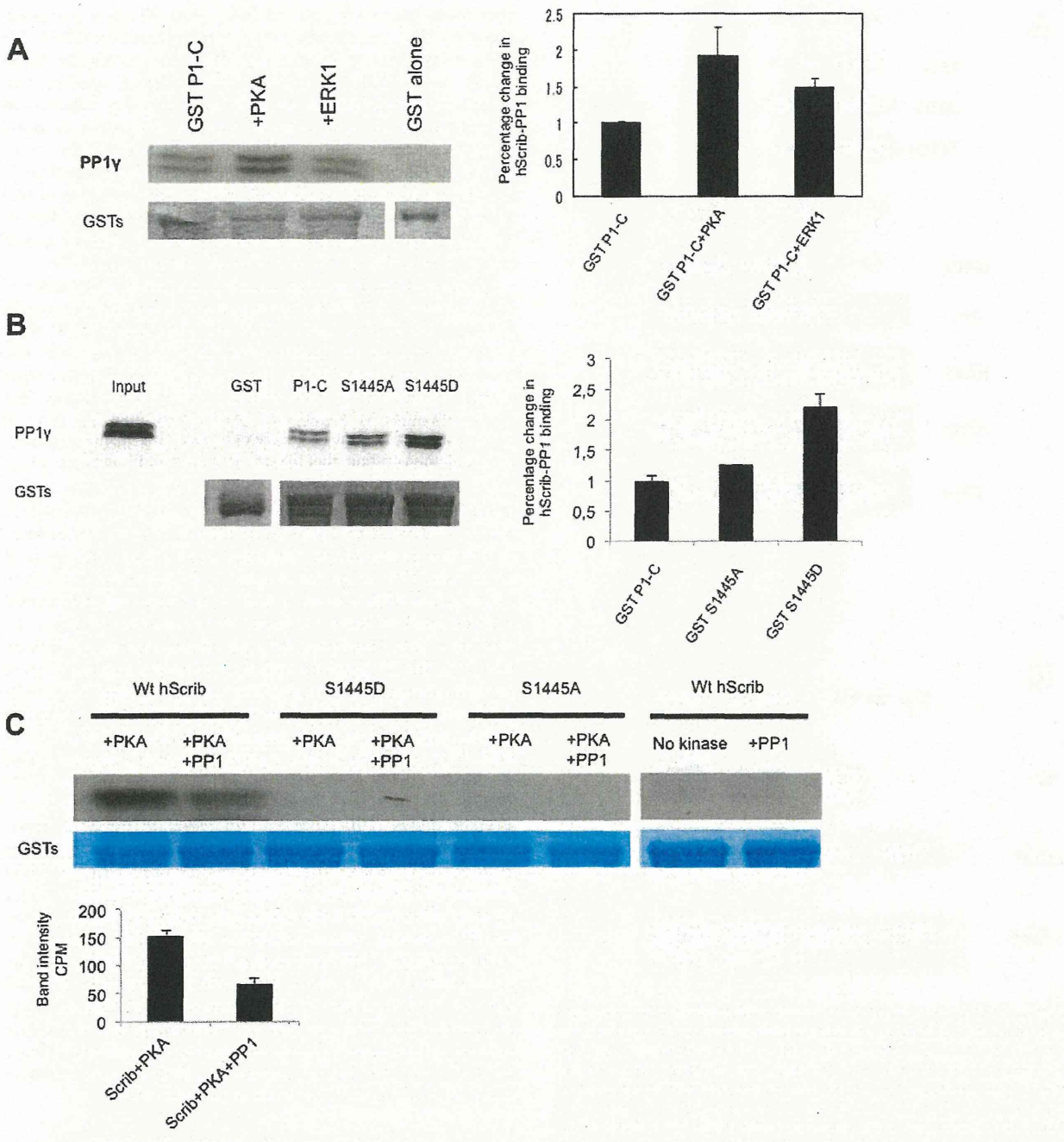

Figure 3. hScrib is a substrate of PP1γ. A) Purified GST-hScrib fusion protein was in vitro phosphorylated with purified PKA or ERK1 as described previously (19) and then incubated with PP1γ for 20 mins at 30°C. Bound PP1γwas detected by western blotting with anti PP1γ antibody. The lower panel shows the ponceau stain of the nitrocellulose, and the upper right panel shows the quantitations from three independent experiments. Note that hScrib phosphorylated by PKA exhibits increased association with PP1γ. B) Purified PP1γ was incubated with purified full length wild type GST-hScrib fusion protein (P1-C), the mutants S1445A, S1445D or GST alone as a control. After extensive washing the bound PP1γ was ascertained by western blotting. The upper panel shows the result of the western blot, with the 20% input of PP1γ also shown for comparison. The lower panel shows the ponceau stain of the nitrocellulose. The histogram shows the quantitation from three independent experiments. C) Purified GST-hScrib wild type and PKA phospho-site mutants of hScrib were in vitro phosphorylated with purified PKA in the presence of radiolabeled ATP as described previously (19) and incubated with PP1γ for 20 mins at 30°C. The remaining level of phosphorylated hScrib was then determined following SDS PAGE and autoradiography. The two right-hand lanes show lack of phosphorylation of hScrib in the absence of PKA, whilst the lower panels show the Coomassie stain of the gel demonstrating equal levels of the GST-hScrib fusion protein throughout. The quantitation of hScrib phosphorylation from three independent experiments is also shown.
doi:10.1371/journal.pone.0053752.g003